Optical scattering on ferrofluid agglomerates

J.-C. Bacri, D. Salin

Classification
Physics Abstracts
61.10D — 75.50M

Optical scattering on ferrofluid agglomerates

J.-C. Bacri and D. Salin

Laboratoire d'Ultrasons (*), Université Pierre et Marie Curie,
Tour 13, 4, place Jussieu, 75230 Paris Cedex 05, France

(*Reçu le 15 juillet 1982, accepté le 23 septembre 1982*)

Résumé. — L'observation directe d'un échantillon mince de ferrofluide soumis à un champ magnétique montre l'existence d'un réseau localement hexagonal d'agglomérats. Nous avons observé la figure de diffraction par ce réseau.

Abstract. — Direct microscopic observation of a thin sample of ionic ferrofluid, in the presence of a magnetic field, shows the existence of a locally hexagonal lattice of agglomerates. We have observed the unusual pattern of the light scattered by this array.

1. **Introduction.** — Ferrofluids are colloidal suspensions of ferromagnetic grains with a typical size of 100 Å. In the presence of a magnetic field, agglomeration phenomena between grains occur [1-3]. The prolate ellipsoid shape [3, 4] of the agglomerates is due to a competition between magnetic energy, which favours elongated agglomerates in the field direction, and surface energy, which favours a spherical shape. Under a given magnetic field the colloidal suspension behaves as an assembly of prolate ellipsoids of nearly the same size and shape [2]. We report here a study of some optical properties of such an assembly of agglomerates when the length 2 a of the ellipsoids is limited by the sample glass boundaries.

2. **Experimental set up.** — We use a ferrofluid obtained through a chemical process without surfactant [5]. The concentration in ionic iron of our ferrofluid suspension is molar. The magnetic-grain diameters are nearly 100 Å and the mean distance between grains is 200 Å. The ferrofluid sample is put in a disc glass cell of diameter 1 cm. The thicknesses e of our different cells are 20, 75, 100, 200 μm. The 350 Oersted magnetic field **H** is applied along the direction of the cell axis and perpendicular to the glass boundaries (Fig. 1). The incoming laser beam (λ = 6 328 Å, beam diameter = 1 mm) has a varying inclination θ_i with the direction of **H**. We observe, on a screen P perpendicular to **H**, the light scattered by the sample. The scattered pattern, in P at a distance L = 9 cm from the sample, is analysed using a 3000 ASA Polaroid film.

3. **Rough experimental results.** — Typical Polaroid pictures of the scattered light are given in four pictures corresponding to the same exposure :

1a : $\theta_i = 0$; the laser beam is in the field direction : we observe a small ring D centred on the laser beam.

1b : $\theta_i = 2°$; the intensity is enhanced on the half ring D while the other part of the ring vanishes.

(*) Associated with the Centre National de la Recherche Scientifique.

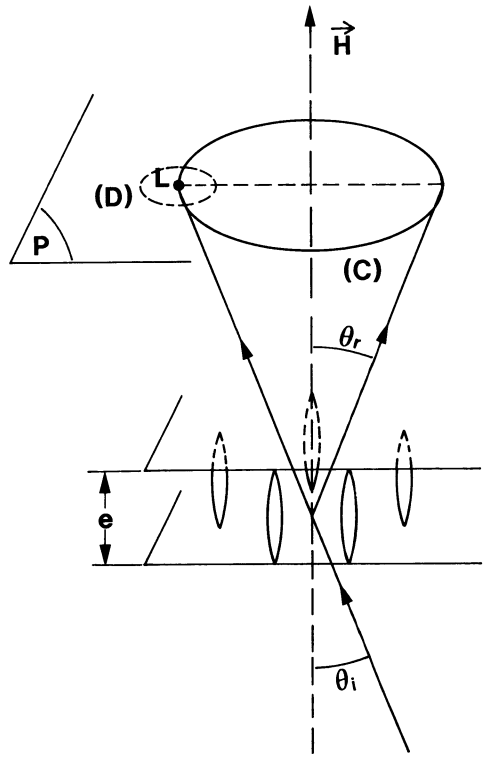

Fig. 1. — Scheme of our experimental set up. θ_i is the variable angle of the incident laser beam with the field direction. P is our plane of observation where pictures are taken.

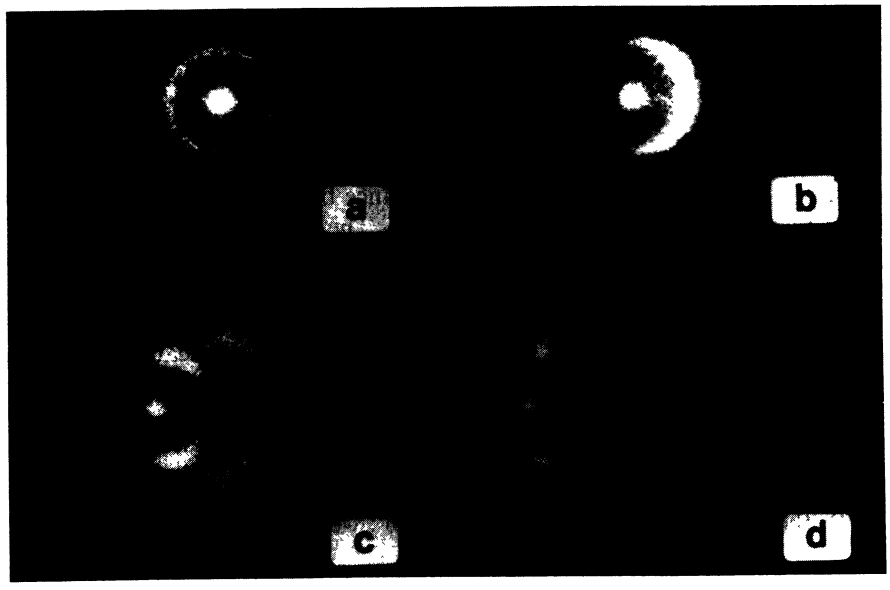

Picture 1. — Pattern of the light scattered by a 75 μm thick sample of ferrofluid in presence of a magnetic field for different incident angle θ_i (Fig. 1) at the same exposure. *a*) $\theta_i = 0$; *b*) $\theta_i = 2°$; *c*) $\theta_i = 8°$; *d*) $\theta_i = 15°$.

1*c* : $\theta_i = 8°$; the moon quarter has been transformed into two orange quarters centred on the laser beam. Another ring (ring C_0) appears centred along the field direction (Fig. 1) and passing through the direct laser beam (L).

1*d* : $\theta_i = 15°$; the initial ring D has achieved its metamorphosis into two enhancements on ring C, which has become thinner.

Picture 2 ($\theta_i = 15°$, $e = 100$ μm) is voluntarily overexposed : we observe a series of rings C_n concentric with ring C_0 with two enhancements on each ring C_n. These enhancements are all on ring D. The experimental features of ring C_0 are :

— for a given θ_i the radius R of circle C_0 is independent of the sample thickness ;

— for a given e, R increases rapidly with θ_i, and when θ_i tends to $\pi/2$ the circle is transformed into a straight line passing through the direct laser beam ($R = \infty$). We have measured the angular radius θ_r (Fig. 1, $\text{tg}\,\theta_r = R/L$) *versus* the incident angle θ_i, for θ_i from $-\pi/4$ to $\pi/4$. We find $\theta_r = \theta_i$: the C_0 ring is the intersection of the plane P perpendicular to **H** with a light-scattered cone of axis **H** and generatrix the incident light beam (SL). The last features of ring C_0 are that the scattered light has the same polarization as the incident light. At a given θ_i the thickness of the ring decreases as e increases. At a given e the thickness of the ring decreases as θ_i increases.

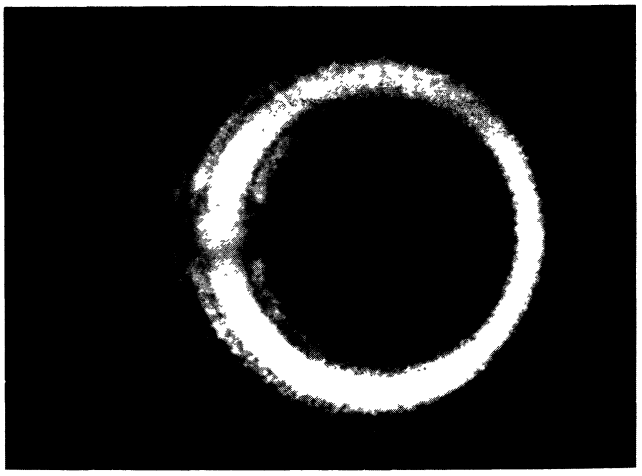

Picture 2. — $\theta_i = 15°$, $e = 100$ μm. The picture is voluntarily overexposed.

Further analysis of our assembly of agglomerates requires a more direct knowledge of our system. We observed our sample through a microscope in the direction of the field (Picture 3) : the different agglomerates of nearly the same size are arranged on a locally hexagonal array. The mean distances d between nearest neighbours are $d = 3$, 5.5, 6.5, 9 μm for sample thicknesses e of respectively 20, 75, 100 and 200 μm. Picture 3 is a top view of our assembly of agglomerates and we do not know from it whether or not the agglomerates are wetting the glass boundaries. This question is answered by picture 4 which shows the behaviour of agglomerates in a glass microcapillary (diameter ~ 50 μm). The field is in the direction of the agglomerates. We clearly see that the agglomerates do not wet the surface and appear as elongated needles close to slender ellipsoids. The glass boundaries push them a few microns away from the surface. The diameter $2b$ of the agglomerates cannot be measured from picture 3 because of optical diffraction. This picture is hazy ; the agglomerates are transformed into spherical drops when the field is turned off. From the measured diameter of the spheres and from volume conservation we get

$$2b = (1 \pm 0.2)\ \mu\text{m} \quad \text{for} \quad e = 75\ \mu\text{m}\,.$$

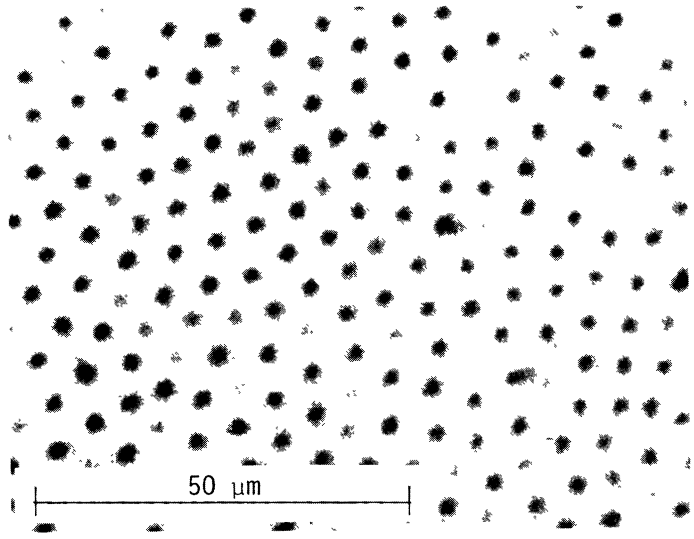

Picture 3. — Microscope picture perpendicular to the field direction of our 75 µm sample.

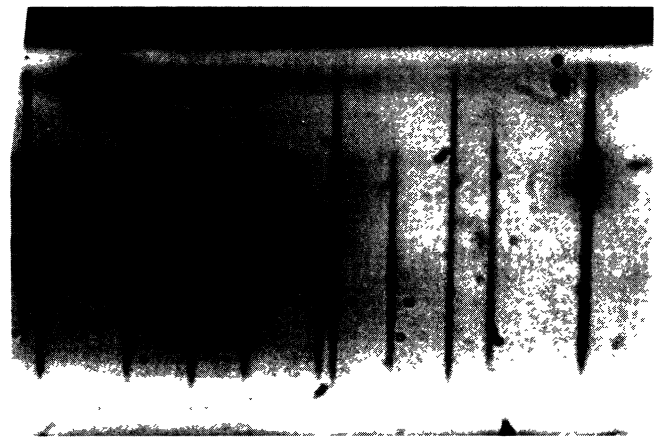

Picture 4. — Microscope picture of agglomerates in a 50 µm diameter microcapillary in presence of a magnetic field perpendicular to the tube axis.

As e increases b also increases ($e = 100$ µm, $2b \simeq 1.5$ µm; $e = 200$ µm, $2b \simeq 3$ µm). Physically each agglomerate behaves as a magnetic dipole parallel to the field direction. The hexagonal array is the result of the repulsive dipolar magnetic interaction between different agglomerates. This array is analogous to the two-dimensional colloidal interfacial crystals [6] where the interaction is a dipole-dipole electrostatic interaction.

4. **Interpretation.** — We will now interpret our optical experiment through an analogy with X-ray diffraction on our sample. For such an analogy, we need the reciprocal lattice [7] of our assembly of agglomerates : from the symmetry of our sample, the reciprocal lattice is one of revolution along the field direction. $\mathbf{k}_i$, $\mathbf{k}_r$, $\mathbf{q}$, are the incident, reflected and diffusion wavevectors, $\mathbf{q} = \mathbf{k}_r - \mathbf{k}_i$. q_z and q_r are respectively the components of $\mathbf{q}$ along and perpendicular to $\mathbf{H}$.

Intensity variations in the reciprocal lattice $\mathcal{R}$ are the result of the form factor F of each individual agglomerate times the interference function I [7] between agglomerates.

We use here the normalized interference function $I_{q=0} = 1$, as in [8]. In the case of elongated ellipsoids ($a/b > 50$) the form factor F is close to that of cylinders (radius b and length $2a$) :

$$F = \left(\frac{\sin q_z a}{(q_z a)}\right)^2 \cdot \left(\frac{J_1(q_r b)}{(q_r b)}\right)^2 \tag{1}$$

J_1 is a Bessel function. The variation of F in the q_z direction is schematized in the insert of figure 2 (at a given q_r) : the plane P_0 ($q_z = 0$) corresponds to a maximum of intensity and secondary maxima are planes P_n parallel to P_0 for wavevectors value $q_z \simeq \pm \left(n + \frac{1}{2}\right)\frac{\pi}{a}$ ($n \neq 0$ is a positive

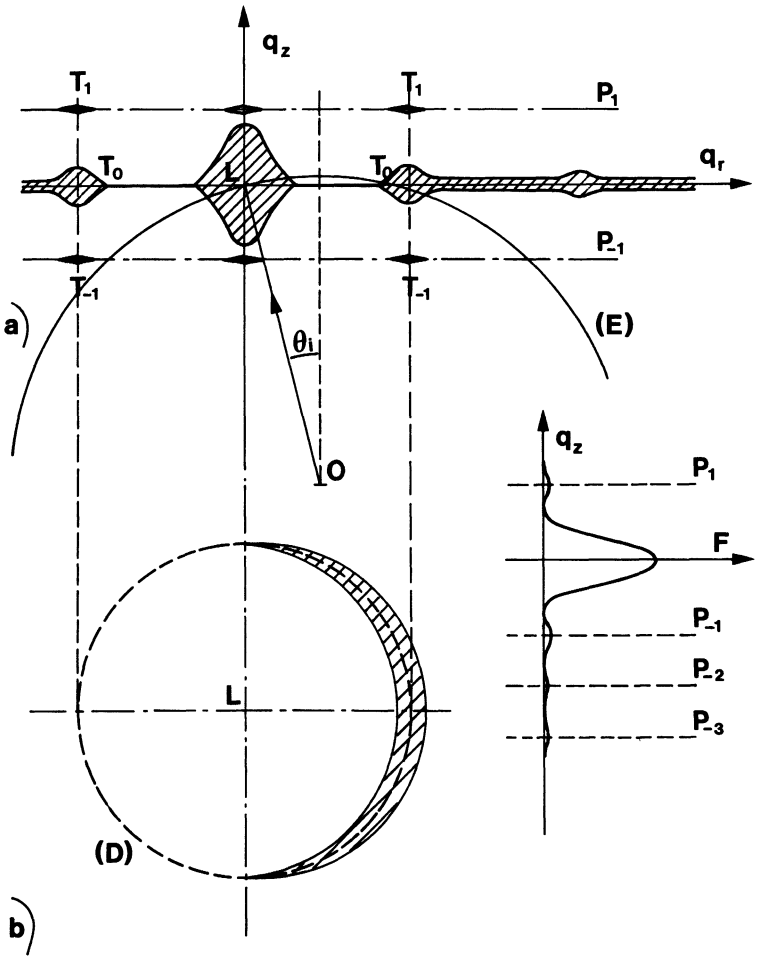

Fig. 2. — *a*) Scheme of the reciprocal lattice $\mathcal{R}$ of our assembly of agglomerates. q_z and q_r are the components, along and perpendicular to the field direction, of the diffusion wavevector. Lines limiting dashed surfaces are equal level of intensity lines. E is the Ewald sphere for a small value of the angle θ_i between the laser beam and the field direction. *b*) Projection of the intersection of $\mathcal{R}$ and E onto a plane perpendicular to **H**. This is indeed the light-scattered pattern we observe. Insert : variation of the form factor F with q_z at a given q_r.

integer). In the q_r direction (perpendicular to **H**) F has its first zero for $q_r\, b \simeq 3.83$. As b is ten times smaller than d, for small values of q_r, intensity variations will be dominated by the effect of the interference function I. In the case of a diatomic-molecule gas I is $[1 + J_0(q_r\, d)]/2$ (d is the interatomic distance) [7]. In our case, with a locally hexagonal array, the interference function given by the seven nearest neighbours is [8] :

$$I = [7 + 24\, J_0(q_r\, d) + 6\, J_0(2\, q_r\, d) + 12\, J_0(\sqrt{3}\, q_r\, d)]/49 \qquad (2)$$

where J_0 is a Bessel function and d is the distance between nearest neighbours. I is maximum for $q_r = 0$ ($I(0) = 1$) and the secondary maximum corresponds to $q_r\, d \simeq 7$. This second maximum is large ($I \sim 0.33$) and there is a wide deep minimum between this maximum and the direct laser beam ($q = 0$). For large values of $q_r\, d$, I tends to 1/7. Notice that even for a liquid-like arrangement (only a mean distance d) the position of the second maximum is close to the value obtained from equation (2) ($q_r\, d \sim 7$) but the relative width and depth of the first minimum increases as the long-range order of the lattice increases. The reciprocal lattice is schematized on figures 2*a* and 3*b* in a plane (q_z, q_r). The line limiting the dashed part of the figure is an (arbitrary) equal level of intensity line of the function F times I. The T_n are the tori corresponding to the second maximum

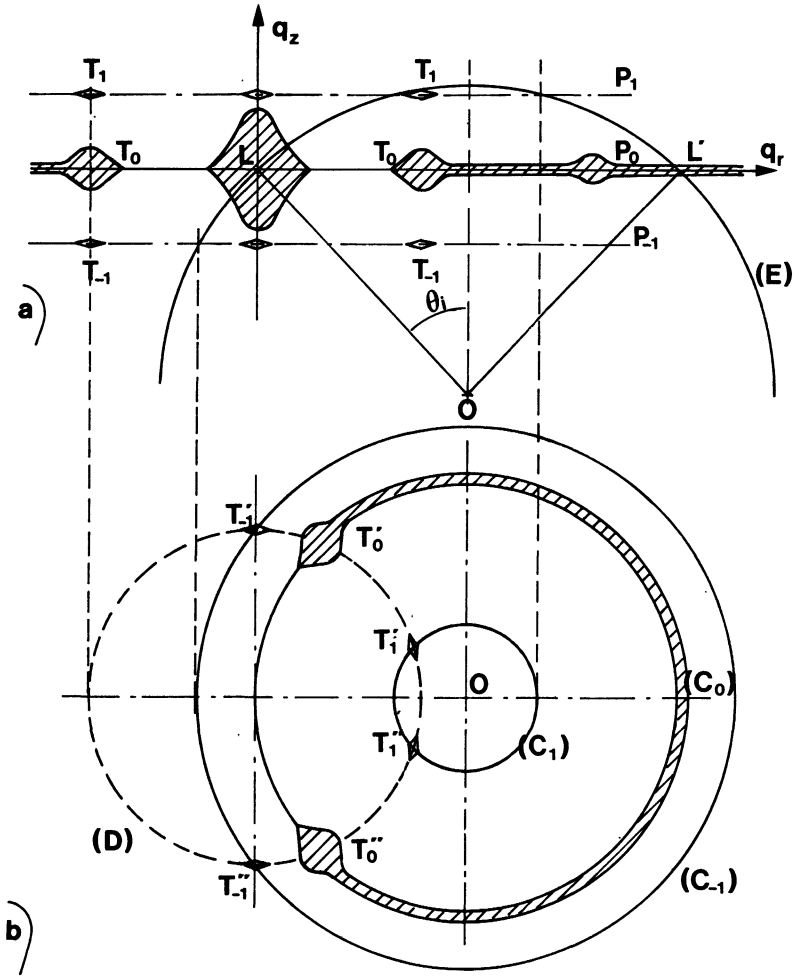

Fig. 3. — *a*) and *b*) are respectively analogous to figures 2*a* and 2*b* but for a much larger incident angle θ_i.

of the interference function (2). The scattered light from the assembly of agglomerates would be observed for **q** values to the intersection of the reciprocal lattice $\mathcal{R}$ with the Ewald sphere E of radius $k = 2\pi/\lambda$, where λ is the laser wavelength. (Because we use wavevectors and not wavenumbers, the radius of our Ewald sphere differs by a factor 2π from the usual value). E passes by the direct laser spot L for all values of the angle θ_i. Figures 2 and 3 correpond to two different values of θ_i. Figures 2*b* and 3*b* are a projection, onto a plane perpendicular to **H**, of the intersection of E with $\mathcal{R}$. (These figures correspond to our plane of observation).

Figure 2 : For small values of θ_i, due to the q_z extension of the torus T_0, the intersection of E and $\mathcal{R}$ occurs on a large part of T_0. Figure 2*b* represents in fact picture 1*b*. Picture 1*a* corresponds to the case $\theta_i = 0$ where E intersects the torus T_0 all around (the intensity is smaller than in 1*b*) : this gives a ring D of diffraction (Debye) of angular radius $\theta_D = (6.5 \pm 0.5)°$. From the value of q_r for the secondary maximum ($q_r d \sim 7$, $\sin\theta_D = q_r/k$) we get a value $d = (6.2 \pm 0.5)$ μm, in reasonable agreement with direct microscope observation $d = (5.5 \pm 0.5)$ μm ($\sim$ 65 agglomerates in a 50 × 50 μm area in picture 3). The evolution from pictures 1*a* to 1*b* shows that, due to the inclination, a part of ring D has its intensity widely enhanced while the other part vanishes.

Figure 3 : For larger values of θ_i the intersection of E with $\mathcal{R}$ occurs mainly in plane P_0 : this gives a circle of light C_0 with two bright spots T'_0 and T''_0 corresponding to the intersection of torus T_0 with E. Figure 3*b* clearly explains pictures 1*c* and 1*d*. Moreover, the sphere E also intersects the different planes P_n along different circles C_n concentric with C_0 : these circles are visible in the overexposed picture 2. The two enhancements on each circle C_n correspond to the intersection of C_n with D (points T'_n and T''_n in figure 3*b*). The fact that the different circles C_n are not equidistant is due to the inclination with which E intersects (Fig. 3*a*) the successive planes P_n. This also explains why the thickness of ring C_0 decreases from picture 1*c* to 1*d*. More quantitatively, the space between different circle allows a measurement of the length $2d$ of the agglomerates ($q_z a = \pm (n + \frac{1}{2})\pi$). We get a value $2a = (90 \pm 10)$ μm in reasonable agreement with the direct microscope observation ($e = 2a$).

5. **Conclusion.** — A thin sample of ionic ferrofluid in the presence of a magnetic field (perpendicular to the sample) exhibits an assembly of pseudo-ellipsoidal agglomerates (rich in magnetic particles) arranged on a locally hexagonal lattice. The few-micron dimensions of the array allow a non-usual light scattered pattern. This kind of experiment is a suitable tool for the study of the dynamics of the hexagonal array formation as a function of an applied magnetic field.

References

[1] PETERSON, E. A. and KRUEGER, D. A., *J. Colloid Interface Sci.* **62** (1977) 24.
[2] LIAO, W. H. and KRUEGER, D. A., *J. Colloid Interface Sci.* **70** (1979) 564.
[3] HAYES, C. G., *J. Colloid Interface Sci.* **52** (1975) 239.
[4] BACRI, J.-C., SALIN, D. and MASSART, R., *J. Physique-Lett.* **43** (1982) L-179.
[5] MASSART, R., *IEEE Trans. Magn.* **17** (1981) 1241.
[6] PIERANSKI, P., *Phys. Rev. Lett.* **45** (1980) 569.
[7] GUINIER, A., *Théorie et technique de la radiocristallographie* (Dunod, Paris) 1956, chapitre 13.
[8] KERKER, M., *The Scattering of Light and other Electromagnetic Radiation* (Academic Press) 1979.